The sensitivity of regional sea level changes to the depth of Antarctic meltwater fluxes

Ian Eisenman[1], Aurora Basinski-Ferris[2], Emma Beer[3], and Laure Zanna[2]

[1]UC San Diego
[2]New York University
[3]Scripps Institution of Oceanography

March 11, 2024

Abstract

Regional patterns of sea level rise are affected by a range of factors including glacial melting, which has occurred in recent decades and is projected to increase in the future, perhaps dramatically. Previous modeling studies have typically included fluxes from melting glacial ice only as a surface forcing of the ocean or as an offline addition to the sea surface height fields produced by climate models. However, observational estimates suggest that the majority of the meltwater from the Antarctic Ice Sheet actually enters the ocean at depth through ice shelf basal melt. Here we use simulations with an ocean general circulation model in an idealized configuration. The results show that the simulated global sea level rise pattern is sensitive to the depth at which Antarctic meltwater enters the ocean. Further analysis suggests that the response is dictated primarily by the steric response to the depth of the meltwater flux.

The sensitivity of regional sea level changes to the depth of Antarctic meltwater fluxes

Ian Eisenman[1], Aurora Basinski-Ferris[2], Emma Beer[3], and Laure Zanna[2]

[1]Scripps Institution of Oceanography, University of California San Diego, La Jolla, CA, USA
[2]Courant Institute of Mathematical Sciences, New York University, New York, NY, USA
[3]Department of Earth, Environmental and Planetary Sciences, Rice University, Houston, TX, USA

Key Points:

- The depth at which Antarctic meltwater enters the ocean influences global sea level rise patterns
- The sea level rise signal tends to travel more slowly when meltwater fluxes occur at depth
- This is dictated primarily by the steric response to the depth of the meltwater fluxes

Corresponding author: Ian Eisenman, `eisenman@ucsd.edu`

Abstract

Regional patterns of sea level rise are affected by a range of factors including glacial melting, which has occurred in recent decades and is projected to increase in the future, perhaps dramatically. Previous modeling studies have typically included fluxes from melting glacial ice only as a surface forcing of the ocean or as an offline addition to the sea surface height fields produced by climate models. However, observational estimates suggest that the majority of the meltwater from the Antarctic Ice Sheet actually enters the ocean at depth through ice shelf basal melt. Here we use simulations with an ocean general circulation model in an idealized configuration. The results show that the simulated global sea level rise pattern is sensitive to the depth at which Antarctic meltwater enters the ocean. Further analysis suggests that the response is dictated primarily by the steric response to the depth of the meltwater flux.

Plain Language Summary

The time-varying pattern of sea level rise is projected to cause some coastal communities to be impacted more than others during the coming century. This is influenced by the melting of Antarctic ice. Previous modeling studies have injected this meltwater at the ocean surface, despite observational evidence suggesting that it enters the ocean primarily at depth. Here we use simulations with a model in an idealized configuration to investigate how the sea level rise pattern depends on the depth at which Antarctic meltwater enters the ocean. We find that the sea level change signal tends to travel more slowly across the global ocean when the meltwater enters the ocean at depth. These results have implications for projected regional sea level changes in response to the melting of Antarctic ice.

1 Introduction

Sea level rise is expected to be a major consequence of global warming, with costs from coastal flooding estimated to reach 3% of global GDP by 2100 (Jevrejeva et al., 2018). This impact depends crucially on the time-varying spatial pattern of future sea level rise. Sea level varies regionally due to factors including surface forcing, ocean circulation changes, thermal expansion of seawater, and melting of glacial ice.

Observational estimates of sea level changes during recent decades show substantial spatial variations (Supporting Information (SI) Fig. S1a). Future projections are also characterized by large spatial variations (SI Fig. S1b), although there is considerable uncertainty in the regional structure of projected sea level rise during the coming century (e.g., Gregory et al., 2016; Couldrey et al., 2023).

The melting of glacial ice influences global and regional sea level changes due to the volume added to the ocean, the effect of the freshwater flux on the ocean salinity, and the effect of latent heat of melting on the ocean temperature if the ice melts in the ocean (e.g., Church et al., 2013). Variations in the distribution of ice on land also influence regional sea level due to changes in the shape of the gravitational field of the Earth (e.g., Bamber et al., 2009; Mitrovica et al., 2009; Gomez et al., 2010).

The Antarctic Ice Sheet is the largest body of frozen ice on earth and contains enough ice to cause a global sea level rise of 60 m. Observational studies have found that the mass of the Antarctic Ice Sheet has decreased during recent decades (e.g., Rignot et al., 2011; Velicogna & Wahr, 2013; Bamber et al., 2018; Rignot et al., 2019; Smith et al., 2020; Otosaka et al., 2023). This is associated with an increase in freshwater discharge into the ocean, which impacts global and regional sea level. Floating ice shelves around Antarctica have also been losing mass during recent decades (Shepherd et al., 2010; Paolo et al., 2015; Rignot et al., 2019). Model projections suggest that the rate of ice mass loss in Antarctica will increase in the future, perhaps dramatically (e.g., Nick et al., 2013; Joughin et al., 2014; DeConto & Pollard, 2016; Edwards et al., 2019; Seroussi et al., 2020).

Freshwater fluxes into the ocean from glacial mass loss are not included in the comprehensive global climate model (GCM) simulations carried out for the Coupled Model Intercomparison Project Phase 5 (CMIP5) and Phase 6 (CMIP6) (Taylor et al., 2011; Eyring et al., 2016), which are used for the future projections in the IPCC Assessment Reports. These GCMs do not resolve ice sheet changes, instead typically representing ice sheets essentially as land with a thick snow cover and routing any excess snow accumulation back to the ocean. For example, in the CMIP5 model NCAR CCSM4, if snow accumulation reaches 1 m of snow water equivalent then any additional snowfall is added as runoff to the ocean surface net freshwater flux near the coast (Oleson et al., 2010).

Future sea level projections in the IPCC AR5 were created from CMIP5 simulation output as the sum of two non-interactive components (Church et al., 2013): (i) the ocean dynamic sea level field plus the global-mean sea level rise due to thermal expansion of the ocean, which is computed in each GCM, and (ii) the sea level change from ice sheets, smaller glaciers, and terrestrial water, which is calculated using a separate modeling framework (note that the GCMs do not simulate changes in ocean volume). The latter is forced by the global-mean temperature from the GCMs, and it accounts for the mass balance of the Antarctic and Greenland Ice Sheets and smaller glaciers, groundwater storage changes, and the regional influence of gravitational and rotational changes. Hence the sea level projection shown in SI Fig. S1, which is equivalent to the projections used in the IPCC AR5, does not include the influence of glacial melt on ocean circulation and dynamic sea level changes. A similar approach is used in the IPCC AR6 based on CMIP6 simulation results.

Previous climate modeling studies that have explicitly included fluxes from Antarctic ice mass loss have typically treated them as part of the surface forcing of the ocean (e.g., Stouffer et al., 2007; Stammer, 2008; Bronselaer et al., 2018; Golledge et al., 2019; Moorman et al., 2020; Park et al., 2023). However, observational evidence suggests that the largest source of ablation in Antarctica is basal melt of ice shelves in contact with the ocean at depth, with a smaller contribution coming from iceberg calving (Rignot et al., 2013; Depoorter et al., 2013). Consistent with this, *in situ* measurements of the water column near an Antarctic ice shelf show that the meltwater is most concentrated near a depth of 0.5 km below the surface (Kim et al., 2016). Furthermore, *in situ* measurements from another study indicate that Antarctic glacial meltwater is often injected into the coastal ocean considerably deeper than the basal melt source due to overturning instability of the outflow from the ice shelf cavity (Garabato et al., 2017). Measurements such as these suggest that a substantial fraction of the meltwater fluxes associated with Antarctic ice mass loss should be applied at a depth greater than 0.5 km below the surface in model projections of sea level rise, since GCMs used for future projections normally do not simulate ice shelf ablation or cavity flow.

The regional sea level response to Antarctic ice melt may be expected to potentially depend on the depth of the forcing, because this forcing can trigger a range of depth-dependent baroclinic responses within the ocean. To this end, a study using satellite measurements together with an ocean model found considerable spatial structure of sea level changes near Antarctica associated with the vertical structure of temperature and salinity variations from the ablation of the ice shelves (Rye et al., 2014). Similarly, an ocean modeling study found that the simulated temperature and salinity along the continental shelf depends on whether Antarctic ice shelf melt fluxes are applied at the surface or at depth (Mathiot et al., 2017).

However, although some previous modeling studies have applied subsurface Antarctic ice shelf melt fluxes to study the response of the Southern Ocean stratification, sea ice cover, and pattern of sea surface temperature changes (Pauling et al., 2016, 2017; Merino

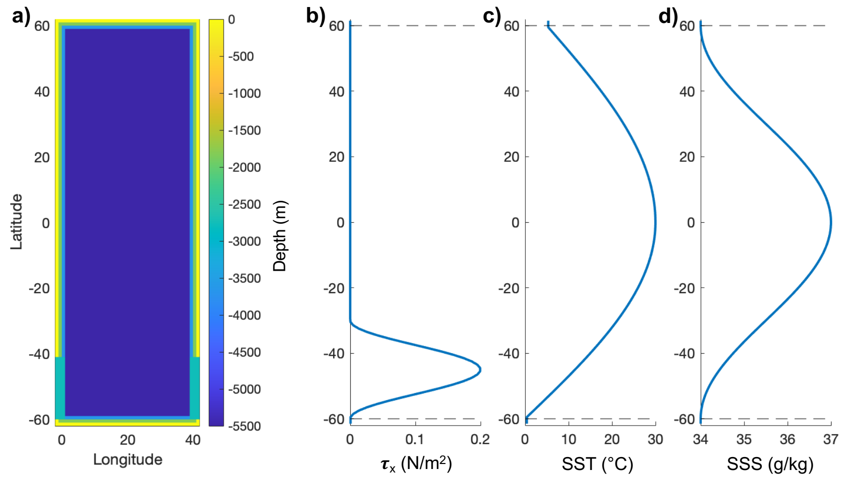

Figure 1. MITgcm simulation setup. (a) Basin bathymetry, including re-entrant Southern Ocean channel. (b) Specified zonal wind stress forcing. (c) Sea surface temperature relaxation field. (d) Sea surface salinity relaxation field. This setup is similar to Munday et al. (2013) but adopts a wider basin and adds continental shelves. During the Spin-up simulation, the temperature and salinity are relaxed to these fields. The relaxation conditions are replaced with specified surface fluxes during the Control and freshwater perturbation simulations following Zika et al. (2018) and Todd et al. (2020).

et al., 2018; Mathiot et al., 2017; Jeong et al., 2020; Dong et al., 2022), there has been a paucity of previous work exploring model simulations of the global sea level response to subsurface ice melt forcing.

Improved understanding of the ocean response to subsurface fluxes from Antarctica can help reduce the uncertainty in the future ocean circulation and climate response to such perturbations. It may also help elucidate the role of sub-surface processes in triggering ice melt feedbacks that have been proposed in recent studies (Schmidtko et al., 2014; Bronselaer et al., 2018; Silvano et al., 2018; Golledge et al., 2019; Si et al., 2023). Here we use ocean GCM simulations in an idealized configuration in order to provide an initial proof-of-concept to demonstrate how the pattern of sea level rise depends on the depth of melt fluxes around Antarctica.

2 Description of simulations

The simulations were carried out with the Massachusetts Institute of Technology General Circulation Model (MITgcm: Marshall et al., 1997) setup in an idealized rectangular ocean basin bathymetry with a re-entrant channel in the Southern Ocean. We begin with a "Spin-up" simulation, in which we use surface temperature and salinity relaxation conditions with relaxation timescales of 10 and 30 days, respectively, as well as specified surface wind stress over the Southern Ocean. The basin configuration and forcing are shown in Fig. 1. We adopt a relatively coarse horizontal resolution of 1°× 1°, using the Gent-McWilliams (GM) parameterization with an eddy thickness diffusivity of 1000 m^{2}s^{-1} to represent unresolved mesoscale eddies. We run the model with constant forcing, rather than including seasonal variations. We use idealized continental shelves along the basin edges, with the bathymetry decreasing linearly from a depth of 0 m to the basin depth of 5500 m over 4 degrees, with no-slip boundary conditions along the walls and bottom of the basin, and we use a channel depth of 2750 m.

The simulations are described in more detail in SI Sec. S1. We branch the "Control", "Surface" freshwater perturbation, and "Deep" freshwater perturbation simulations from the approximately equilibrated state at the beginning of year 7540 of the Spin-up simulation (note that the simulations start at the beginning of year 0). These simulations have the temperature and salinity relaxation condition replaced by specified temperature and salinity fluxes, using a repeating 60-year cycle of daily fluxes that we save from years 7540-7599 of the Spin-up simulation. This follows the method of Zika et al. (2018) and Todd et al. (2020), allowing us to directly examine the response of the ocean to perturbations without damping by the atmosphere. The Control simulation has no freshwater perturbation and hence is similar to the Spin-up simulation, except that it has fixed surface fluxes rather than relaxation conditions. The Surface and Deep simulations have freshwater perturbations as described below. We run each of these three fixed-flux simulations for 240 years while also continuing the Spin-up simulation for 435 years to the end of year 7974.

Some previous studies of the ocean response to Antarctic ice melt have applied a horizontal structure of the meltwater flux that is uniform around the Antarctic coast (e.g., Bronselaer et al., 2018), others have scaled the observed pattern (e.g., Snow et al., 2016), and others have used more sophisticated representations such as scaling the linear trend of recent observed ice shelf thickness changes (Moorman et al., 2020). Each of these approaches has strengths and weaknesses. Using a horizontally-uniform forcing is simple and hence conducive to building conceptual understanding, but it may miss key features of the horizontal structure of the ice melt forcing. Scaling observed fluxes could be more accurate, but the fluxes from ice shelves with the largest basal melt rates today will not necessarily increase the most in the future. Amplifying observed ice shelf thickness changes may better capture these sensitivities, but the observational record may be too short to separate interannual variability in basal melt from secular trends, and ice shelf thickness changes do not directly map to basal melt changes due to factors including changes in ice flow across the grounding line (e.g., Adusumilli et al., 2020).

In the present study, we apply meltwater fluxes in zonally-uniform bands along the southern border of the basin (60°S), with the aim of providing a first step toward understanding how the sea level adjustment depends on the depth of the flux. The Surface simulation has a 0.1 Sv freshwater flux applied at the surface, and the Deep simulation has a 0.1 Sv freshwater flux applied at a depth of 1 km. The fluxes are held constant throughout the simulations. We do not include cooling from the latent heat of ice shelf melting. This 0.1 Sv flux is similar to the Antarctic Ice Sheet meltwater discharge rates in some projections. Edwards et al. (2019) report an 83 cm Antarctic contribution to sea level during 2000-2100, and DeConto and Pollard (2016) similarly report a 105 cm Antarctic contribution to sea level during 2000-2100, where in both cases we are citing the highest reported scenarios, which use RCP8.5 forcing and include the marine ice cliff instability. These amount to century-averaged freshwater inputs of 0.091 Sv and 0.12 Sv, respectively. The DeConto and Pollard (2016) ice sheet simulation has similarly been used for the forcing in a number of other ocean modeling studies (e.g., Bronselaer et al., 2018; Lago & England, 2019; Schloesser et al., 2019). Note that this imposed 0.1 Sv flux anomaly is about twice as large as the Antarctic Ice Sheet basal melt rate in the current climate, which is estimated by Rignot et al. (2013) to be 1325 gigatons per year, amounting to a freshwater flux of 0.042 Sv. Estimates of future Antarctic meltwater fluxes are subject to uncertainty in the ice sheet model physics, including the hypothesized marine ice cliff instability process, as well as uncertainty in the future radiative forcing scenario. Here we adopt a value on the high side of the uncertainty range in order to emphasize the possible sensitivity to meltwater depth.

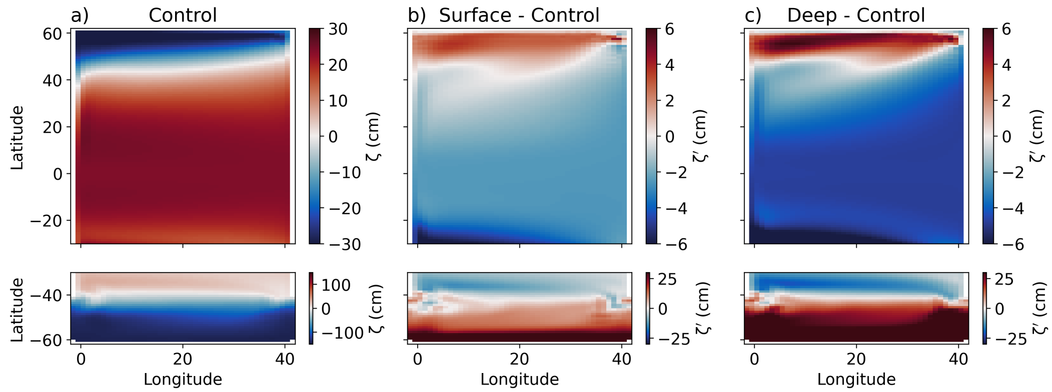

Figure 2. Ocean dynamic sea level ζ. (a) Control simulation. (b) Surface freshwater perturbation simulation anomaly from Control. (c) Deep freshwater perturbation simulation anomaly from Control. The fields are averaged over the last decade of each of the 240-year simulations.

3 Results

We focus on the ocean dynamic sea level ζ, which is the regional pattern of sea surface height; it is defined as the departure from the geoid, with a global-mean value of zero. This is equivalent to the MITgcm output variable "Eta" with the global-mean value removed. Note that ζ is reported in CMIP5 and CMIP6 as the simulation output variable "zos".

The dynamic sea level ζ in the Control simulation is shown in Fig. 2a. It is positive at latitudes equatorward of about 40°N and 40°S and negative at higher latitudes, which qualitatively resembles the observed global ocean (e.g., Mulet et al., 2021, their Fig. 6a).

The dynamic sea level anomalies from the Control simulations, ζ', are plotted for the Surface and Deep simulations in Fig. 2b,c. The constant freshwater fluxes applied at the southern edge of the basin in both simulations leads to a higher regional sea level in southern high latitudes, and it broadly causes a reduction in the amplitude of the spatial pattern of ζ in the Control simulation. The key difference between the two simulations is that after the first couple decades, ζ' remains lower in the Northern Hemisphere and higher in the Southern Hemisphere in the Deep simulation, indicating that the applied freshwater flux is spreading more slowly across the ocean basin.

This can be seen clearly in line plots of ζ' averaged spatially over each hemisphere (Fig. 3). Averaged over the final 200 years of the simulations, ζ' is 2.9 cm higher in the Southern Hemisphere than in the Northern Hemisphere in the Deep simulation, compared with just 1.8 cm in the Surface simulation. Note that since ζ is defined to have a global-mean value of zero, the value in the Northern Hemisphere is equal and opposite to the value in the Southern Hemisphere.

The results in Figs. 2 and 3 show that the global sea level change pattern depends critically on the depth of the Antarctic meltwater perturbation, with far field sea level differences that persist throughout the simulations. Broadly, the elevated regional sea level moves more slowly out of the Southern Hemisphere when the freshwater is injected at depth.

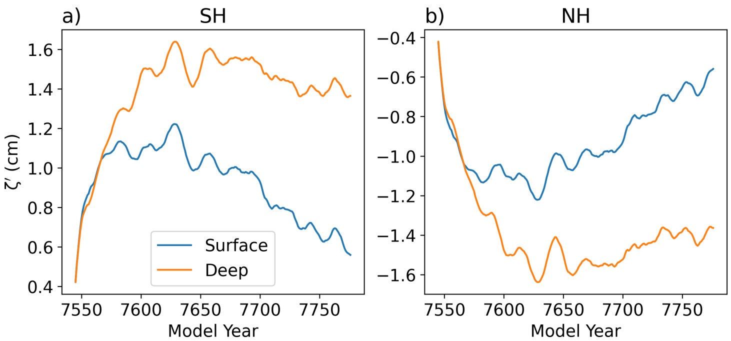

Figure 3. Time series of dynamic sea level anomaly from the Control simulation, ζ', in the Surface and Deep simulations. (a) Southern Hemisphere spatial mean. (b) Northern Hemisphere spatial mean. All curves are smoothed with a 10-year running mean.

4 Sea level change decomposition

The dynamic sea level pattern in each perturbed simulation (Surface or Deep) can be decomposed as follows (e.g., Gill & Niiler, 1973; Yin et al., 2010; Griffies et al., 2014; Gregory et al., 2019):

$$\zeta' = \underbrace{\frac{p_b'}{\rho_0\, g}}_{\text{Mass}} - \underbrace{\frac{1}{\rho_0}\int_{-H}^{\zeta-B} \rho'\, dz}_{\text{Steric}}, \tag{1}$$

where ρ is the ocean density field, ρ_0 is the ocean reference density, g is the acceleration of gravity, p_b is the ocean bottom hydrostatic pressure, H is the ocean depth, and B represents the inverse barometer correction due to variations in sea level pressure (adopting the terminology of Gregory et al., 2019). Here primed quantities represent the anomaly in a perturbed simulation relative to the Control simulation, with the global mean removed. Note that Eq. (1) is derived from the hydrostatic balance with the near-surface density approximated to be ρ_0 (e.g., Yin et al., 2010, their Sec. 2b).

The first term on the right-hand side of Eq. (1) captures sea level increases due to seawater being added to the column, i.e., it represents ocean mass redistribution. The second term on the right-hand side of Eq. (1) captures sea level increases due to the column becoming less dense without changing its mass, i.e., it represents the sea level change from local steric changes in the density field. Note that in Boussinesq models such as MITgcm the steric term is not a true expansion or contraction, but it does influence the simulated currents.

The first term is approximately associated with the barotropic component of the flow, and the second term is approximately associated with the baroclinic component of the flow (e.g., Savage et al., 2017). Explicitly decomposing the sea level changes into components associated with the barotropic and baroclinic components of the flow, following the method of McWilliams et al. (2023), leads to qualitatively similar results (Fig. S4).

Freshwater injection causes an increase in mass, which leads to a positive contribution to local sea level from the mass term in Eq. (1). This increase in sea level is mitigated by the column becoming less dense due to the reduction in salinity from the freshwater injection, which leads to a negative contribution to local sea level from the steric term in Eq. (1).

The terms in Eq. (1) can be readily computed from the MITgcm simulation output. The left-hand side is the difference in the dynamic sea level ζ between the perturbed

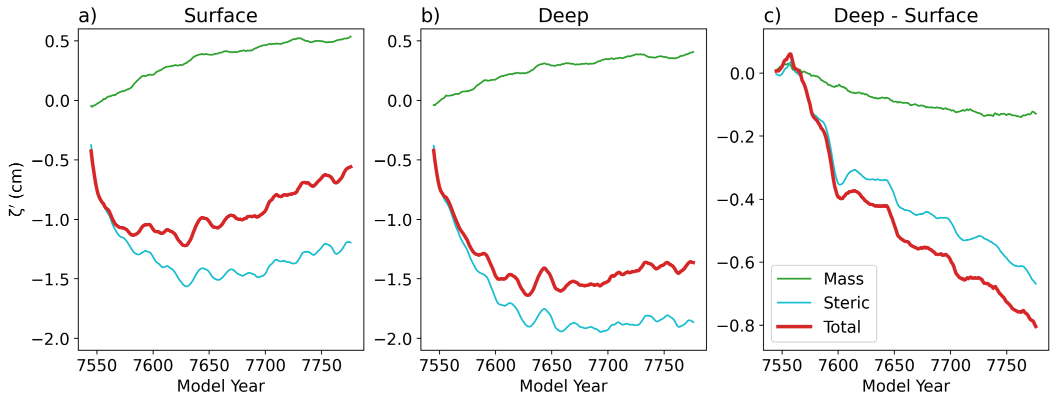

Figure 4. Decomposition of Northern Hemisphere dynamic sea level anomaly ζ' into mass redistribution and steric contributions (Eq. (1)). (a) Surface simulation. (b) Deep simulation. (c) Difference between the two simulations. All curves are smoothed with a 10-year running mean.

simulation and the Control simulation. The mass term is computed using the hydrostatic relationship as the difference between the perturbed simulations in the quantity $\frac{1}{\rho_0}\int_{-H}^{\eta} \rho\, dz$; here, the global mean is removed after calculating this term for each simulation. Since the surface pressure is constant in the MITgcm simulations, we take $B = 0$, and the steric term is computed as $\frac{1}{\rho_0}\int_{-H}^{\zeta} \rho'\, dz$, with ρ' defined as above and ζ the dynamic sea level in the perturbed simulation.

The resulting quantities, averaged over the Northern Hemisphere, are plotted in Fig. 4. Since the dynamic sea level is higher in the hemisphere where freshwater is continuously injected, ζ' is negative in the Northern Hemisphere in both perturbed simulations (Fig. 3). This is associated primarily with the steric term, which explains most of the dynamic sea level anomaly ζ' (Fig. 4). The mass term, by contrast, is relatively small in both perturbed simulations, indicating that this component of the dynamic sea level spreads rapidly across the globe (Fig. 4), consistent with the rapid propagation of barotropic waves.

As noted above, the difference in ζ' between the two hemispheres is larger in the Deep simulation, consistent with the injected freshwater flux spreading more slowly across the basin. The decomposition shows that this difference occurs primarily due to the steric term (Fig. 4). Although the mass from the injected freshwater spreads quickly into the Northern Hemisphere in both simulations (near-zero values of green curves in Fig. 4), the density change from the injected freshwater spreads more slowly (substantial negative values of blue curves in Fig. 4), especially in the Deep simulation.

5 Summary and conclusions

Previous climate modeling studies that have explicitly included fluxes from Antarctic ice mass loss have typically treated them as part of the surface forcing of the ocean. However, observational estimates suggest that the largest source of ablation in Antarctica is basal melt of ice shelves, with the freshwater entering the ocean considerably below the surface. In the present study, we use MITgcm simulations of an idealized ocean basin with freshwater injected at the surface or at depth in southern high latitudes. The results suggest that the global sea level change pattern is sensitive to the depth of the Antarctic meltwater perturbation. When the fluxes are applied at depth the signal tends to travel more slowly to the Northern Hemisphere. This is consistent with expectations that the propagation speeds of baroclinic waves will depend on the stratification which is influenced by the depth of the meltwater injection. A decomposition of the sea level changes shows that the sensitivity to meltwater depth occurs primarily due to differences in the baroclinic response.

Many factors have been neglected in these idealized simulations, including the influence of realistic basin geometry, the detailed spatial and temporal structure of the meltwater injection, and the latent heat flux in addition to freshwater injection associated with ice shelf basal melt. Further research into how these factors would influence the result is called for. The simulations were carried out with a 1° GCM, raising important questions about how the results may differ in a higher-resolution model. Furthermore, the scale of the regional patterns of change in the simulation results (Fig. 2c), while of a similar order of magnitude to the projected regional pattern of sea level rise during the coming century (SI Fig. S1), would be considerably smaller than the global-mean sea level rise due to substantial Antarctic Ice Sheet melting. This is true in general for local patterns of dynamic sea level compared to global mean sea level change. Nonetheless, the results presented here suggest that sea level changes are sensitive to the depth of freshwater injections, which suggests that capturing the depth of Antarctic ice shelf meltwater may lead to more accurate projections of future regional sea level changes, in particular when considering local impacts such as increased risk of flooding and storm surge.

Open Research Section

All relevant MITgcm simulation output will be posted on FigShare, and all relevant analysis code will be posted on GitHub, by the time of publication.

Acknowledgments

This work was supported by National Science Foundation grants OCE-2048590 and OCE-2048576.

References

Adusumilli, S., Fricker, H. A., Medley, B., Padman, L., & Siegfried, M. R. (2020). Interannual variations in meltwater input to the Southern Ocean from Antarctic ice shelves. *Nature Geoscience*, 191–194. doi: 10.1038/s41561-020-0616-z

Bamber, J. L., Riva, R. E. M., Vermeersen, B. L. A., & LeBrocq, A. M. (2009). Reassessment of the potential sea-level rise from a collapse of the West Antarctic Ice Sheet. *Science*, *324*(5929), 901–903. doi: 10.1126/science.1169335

Bamber, J. L., Westaway, R. M., Marzeion, B., & Wouters, B. (2018). The land ice contribution to sea level during the satellite era. *Environmental Res. Lett.*, *13*(9), 063008. doi: 10.1088/1748-9326/aadb2c

Bronselaer, B., Winton, M., Griffies, S. M., Hurlin, W. J., Rodgers, K. B., Sergienko, O. V., … Russell, J. L. (2018). Change in future climate due to Antarctic meltwater. *Nature*, *564*(7734), 53–58. doi: 10.1038/s41586-018-0712-z

Church, J., Clark, P., Cazenave, A., Gregory, J., Jevrejeva, S., Levermann, A., … Unnikrishnan, A. (2013). Chapter 13, Sea level change. In T. Stocker et al. (Eds.), *Climate Change 2013: The Physical Science Basis. Contribution of Working Group I to the Fifth Assessment Report of the Intergovernmental Panel on Climate Change.* Cambridge University Press, Cambridge, UK.

Couldrey, M. P., Gregory, J. M., Dong, X., Garuba, O., Haak, H., Hu, A. X., … Zanna, L. (2023). Greenhouse-gas forced changes in the Atlantic meridional overturning circulation and related worldwide sea-level change. *Climate Dynam.*, *60*(7-8), 2003–2039. doi: 10.1007/s00382-022-06386-y

DeConto, R. M., & Pollard, D. (2016). Contribution of Antarctica to past and future sea-level rise. *Nature*, *531*(7596), 591–597. doi: 10.1038/nature17145

Depoorter, M. A., Bamber, J. L., Griggs, J. A., Lenaerts, J. T. M., Ligtenberg, S. R. M., van den Broeke, M. R., & Moholdt, G. (2013). Calving fluxes and basal melt rates of Antarctic ice shelves. *Nature*, *502*(7469), 89–92. doi: 10.1038/nature12567

Dong, Y., Pauling, A. G., Sadai, S., & Armour, K. C. (2022). Antarctic Ice-Sheet meltwater reduces transient warming and climate sensitivity through the sea-surface temperature pattern effect. *Geophys. Res. Lett.*, *49*(24), e2022GL101249. doi: 10.1029/2022GL101249

Ducet, N., Traon, P. Y. L., & Reverdin, G. (2000). Global high-resolution mapping of ocean circulation from TOPEX/Poseidon and ERS-1 and -2. *J. Geophys. Res.*, *105*(C8), 19477–19498. ((AVISO Ssalto/Duacs monthly data accessed from https://www.aviso.altimetry.fr/en/data/data-access.html)) doi: 10.1029/2000JC900063

Edwards, T. L., Brandon, M. A., Durand, G., Edwards, N. R., Golledge, N. R., Holden, P. B., . . . Wernecke, A. (2019). Revisiting Antarctic ice loss due to marine ice-cliff instability. *Nature*, *566*(7742), 58–64. doi: 10.1038/s41586-019-0901-4

Eyring, V., Bony, S., Meehl, G. A., Senior, C. A., Stevens, B., Stouffer, R. J., & Taylor, K. E. (2016). Overview of the Coupled Model Intercomparison Project Phase 6 (CMIP6) experimental design and organization. *Geoscientific Model Development*, *9*(5), 1937–1958. doi: 10.5194/gmd-9-1937-2016

Garabato, A. C. N., Forryan, A., Dutrieux, P., Brannigan, L., Biddle, L. C., Heywood, K. J., . . . Kimura, S. (2017). Vigorous lateral export of the meltwater outflow from beneath an Antarctic ice shelf. *Nature*, *542*(7640), 219–222. doi: 10.1038/nature20825

Gill, A. E., & Niiler, P. P. (1973). Theory of seasonal variability in ocean. *Deep-sea Res.*, *20*(2), 141–177. doi: 10.1016/0011-7471(73)90049-1

Golledge, N. R., Keller, E. D., Gomez, N., Naughten, K. A., Bernales, J., Trusel, L. D., & Edwards, T. L. (2019). Global environmental consequences of twenty-first-century ice-sheet melt. *Nature*, *566*(7742), 65–72. doi: 10.1038/s41586-019-0889-9

Gomez, N., Mitrovica, J. X., Huybers, P., & Clark, P. U. (2010). Sea level as a stabilizing factor for marine-ice-sheet grounding lines. *Nature Geoscience*, *3*(12), 850–853. doi: 10.1038/NGEO1012

Gregory, J., Bouttes, N., Griffies, S. M., Haak, H., Hurlin, W. J., Jungclaus, J., . . . Winton, M. (2016). The Flux-Anomaly-Forced Model Intercomparison Project (FAFMIP) contribution to CMIP6: investigation of sea-level and ocean climate change in response to CO2 forcing. *Geoscientific Model Development*, *9*(11), 3993–4017. doi: 10.5194/gmd-9-3993-2016

Gregory, J., Griffies, S., Hughes, C., Lowe, J., Church, J., Fukimori, I., . . . van de Wal, R. (2019). Concepts and terminology for sea level: Mean, variability and change, both local and global. *Surv. Geophys.*, 1–39. doi: 10.1007/s10712-019-09525-z

Griffies, S. M., Yin, J. J., Durack, P. J., Goddard, P., Bates, S. C., Behrens, E., . . . Zhang, X. B. (2014). An assessment of global and regional sea level for years 1993-2007 in a suite of interannual CORE-II simulations. *Ocean Modelling*, *78*, 35–89. doi: 10.1016/j.ocemod.2014.03.004

Jeong, H., Asay-Davis, X. S., Turner, A. K., Comeau, D. S., Price, S. F., Abernathey, R. P., . . . Ringler, T. D. (2020). Impacts of Ice-Shelf Melting on Water-Mass Transformation in the Southern Ocean from E3SM simulations. *J. Climate*, *33*(13), 5787–5807. doi: 10.1175/JCLI-D-19-0683.1

Jevrejeva, S., Jackson, L. P., Grinsted, A., Lincke, D., & Marzeion, B. (2018). Flood damage costs under the sea level rise with warming of 1.5 degrees C and 2 degrees C. *Environmental Res. Lett.*, *13*(7), 074014. doi: 10.1088/1748-9326/aacc76

Joughin, I., Smith, B. E., & Medley, B. (2014). Marine ice sheet collapse potentially under way for the Thwaites Glacier Basin, West Antarctica. *Science*, *344*(6185), 735–738. doi: 10.1126/science.1249055

Killworth, P. D. (1996). Time interpolation of forcing fields in ocean models. *J. Phys. Oceanogr.*, *26*(1), 136–143. doi: 10.1175/1520-0485(1996)026¡0136:TIOFFI¿2.0.CO;2

Kim, I., Hahm, D., Rhee, T. S., Kim, T. W., Kim, C. S., & Lee, S. (2016). The distribution of glacial meltwater in the Amundsen Sea, Antarctica, revealed by dissolved helium and neon. *J. Geophys. Res.*, *121*(3), 1654–1666. doi: 10.1002/2015JC011211

Lago, V., & England, M. H. (2019). Projected slowdown of Antarctic Bottom Water formation in response to amplified meltwater contributions. *J. Climate*, *32*(19), 6319–6335. doi: 10.1175/JCLI-D-18-0622.1

Marshall, J., Adcroft, A., Hill, C., Perelman, L., & Heisey, C. (1997). A finite-volume, incompressible Navier Stokes model for studies of the ocean on parallel computers. *J. Geophys. Res.*, *102*(C3), 5753–5766. doi: 10.1029/96JC02775

Mathiot, P., Jenkins, A., Harris, C., & Madec, G. (2017). Explicit representation and parametrised impacts of under ice shelf seas in the z* coordinate ocean model NEMO 3.6. *Geoscientific Model Development*, *10*(7), 2849–2874. doi: 10.5194/gmd-10-2849-2017

McWilliams, J. C., Molemaker, J., & Damien, P. (2023). Baroclinic sea-level. *ESS Open Archive*. doi: 10.22541/essoar.169272214.48059542/v1

Merino, N., Jourdain, N. C., Sommer, J. L., Goosse, H., Mathiot, P., & Durand, G. (2018). Impact of increasing Antarctic glacial freshwater release on regional sea-ice cover in the Southern Ocean. *Ocean Modelling*, *121*, 76–89. doi: 10.1016/j.ocemod.2017.11.009

Mitrovica, J. X., Gomez, N., & Clark, P. U. (2009). The sea-level fingerprint of West Antarctic collapse. *Science*, *323*(5915), 753–753. doi: 10.1126/science.1166510

Moorman, R., Morrison, A., & Hogg, A. (2020). Thermal responses to Antarctic Ice Shelf melt in an eddy-rich global ocean-sea ice model. *J. Climate*, *33*(15), 6599–6620. doi: 10.1175/JCLI-D-19-0846.1

Mulet, S., Rio, M.-H., Etienne, H., Artana, C., Cancet, M., Dibarboure, G., … Strub, P. T. (2021). The new CNES-CLS18 global mean dynamic topography. *Ocean Science*, *17*(3), 789–808. Retrieved from `https://os.copernicus.org/articles/17/789/2021/` doi: 10.5194/os-17-789-2021

Munday, D. R., Johnson, H. L., & Marshall, D. P. (2013). Eddy saturation of equilibrated circumpolar currents. *J. Phys. Oceanogr.*, *43*(3), 507–532. doi: 10.1175/JPO-D-12-095.1

Nick, F. M., Vieli, A., Andersen, M. L., Joughin, I., Payne, A., Edwards, T. L., … van de Wal, R. S. W. (2013). Future sea-level rise from Greenland's main outlet glaciers in a warming climate. *Nature*, *497*(7448), 235–238. doi: 10.1038/nature12068

Oleson, K. W., Lawrence, D. M., Bonan, G. B., Flanner, M. G., Kluzek, E., Lawrence, P. J., … Thornton, P. E. (2010). Technical description of version 4.0 of the community land model (clm) [Computer software manual]. National Center for Atmospheric Research, Boulder, CO, http://www.cesm.ucar.edu/models/cesm2/land/CLM50_Tech_Note.pdf.

Otosaka, I. N., Shepherd, A., Ivins, E. R., Schlegel, N. J., Amory, C., van den Broeke, M. R., … Wouters, B. (2023). Mass balance of the Greenland and Antarctic ice sheets from 1992 to 2020. *Earth System Sci. Data*, *15*(4), 1597–1616. doi: 10.5194/essd-15-1597-2023

Paolo, F. S., Fricker, H. A., & Padman, L. (2015). Volume loss from Antarctic ice shelves is accelerating. *Science*, *348*(6232), 327–331. doi: 10.1126/science.aaa0940

Park, J. Y., Schloesser, F., Timmermann, A., Choudhury, D., Lee, J. Y., & Nellikkattil, A. B. (2023). Future sea-level projections with a coupled atmosphere-ocean-ice-sheet model. *Nature Comm.*, *14*(1), 636. doi: 10.1038/s41467-023-36051-9

Pauling, A. G., Bitz, C. M., Smith, I. J., & Langhorne, P. J. (2016). The response of the Southern Ocean and Antarctic sea ice to freshwater from ice shelves in an earth system model. *J. Climate*, *29*(5), 1655–1672. doi: 10.1175/JCLI-D-15-0501.1

Pauling, A. G., Smith, I. J., Langhorne, P. J., & Bitz, C. M. (2017). Time-dependent freshwater input from ice shelves: Impacts on Antarctic sea ice and the Southern Ocean in an earth system model. *Geophys. Res. Lett.*, *44*(20), 10454–10461. doi: 10.1002/2017GL075017

Rignot, E., Jacobs, S., Mouginot, J., & Scheuchl, B. (2013). Ice-shelf melting around Antarctica. *Science*, *341*(6143), 266–270. doi: 10.1126/science.1235798

Rignot, E., Mouginot, J., Scheuchl, B., van den Broeke, M., van Wessem, M. J., & Morlighem, M. (2019). Four decades of Antarctic Ice Sheet mass balance from 1979-2017. *Proc. Natl. Acad. Sci. U.S.A.*, *116*(4), 1095–1103. doi: 10.1073/pnas.1812883116

Rignot, E., Velicogna, I., van den Broeke, M. R., Monaghan, A., & Lenaerts, J. (2011). Acceleration of the contribution of the Greenland and Antarctic ice sheets to sea level rise. *Geophys. Res. Lett.*, *38*, L05503. doi: 10.1029/2011GL046583

Rye, C. D., Garabato, A. C. N., Holland, P. R., Meredith, M. P., Nurser, A. J. G., Hughes, C. W., … Webb, D. J. (2014). Rapid sea-level rise along the Antarctic margins in response to increased glacial discharge. *Nature Geoscience*, *7*(10), 732–735. doi: 10.1038/NGEO2230

Savage, A. C., Arbic, B. K., Richman, J. G., Shriver, J. F., Alford, M. H., Buijsman, M. C., … Zamudio, L. (2017). Frequency content of sea surface height variability from internal gravity waves to mesoscale eddies. *Journal of Geophysical Research: Oceans*, *122*(3), 2519-2538. Retrieved from `https://agupubs.onlinelibrary.wiley.com/doi/abs/10.1002/2016JC012331` doi: https://doi.org/10.1002/2016JC012331

Schloesser, F., Friedrich, T., Timmermann, A., DeConto, R. M., & Pollard, D. (2019). Antarctic iceberg impacts on future Southern Hemisphere climate. *Nature Climate Change*, *9*(9), 672–677. doi: 10.1038/s41558-019-0546-1

Schmidtko, S., Heywood, K. J., Thompson, A. F., & Aoki, S. (2014). Multidecadal warming of Antarctic waters. *Science*, *346*(6214), 1227–1231. doi: 10.1126/science.1256117

Seroussi, H., Nowicki, S., Payne, A. J., Goelzer, H., Lipscomb, W. H., Abe Ouchi, A., … Zwinger, T. (2020). ISMIP6 Antarctica: a multi-model ensemble of the Antarctic ice sheet evolution over the 21st century. *The Cryosphere Discussions*, *2020*, 1–54. doi: 10.5194/tc-2019-324

Shepherd, A., Wingham, D., Wallis, D., Giles, K., Laxon, S., & Sundal, A. V. (2010). Recent loss of floating ice and the consequent sea level contribution. *Geophys. Res. Lett.*, *37*, L13503. doi: 10.1029/2010GL042496

Si, Y. D. F., Stewart, A. L., & Eisenman, I. (2023). Heat transport across the Antarctic Slope Front controlled by cross-slope salinity gradients. *Sci. Adv.*, *9*(18), eadd7049. doi: 10.1126/sciadv.add7049

Silvano, A., Rintoul, S. R., Pena-Molino, B., Hobbs, W. R., van Wijk, E., Aoki, S., … Williams, G. D. (2018). Freshening by glacial meltwater enhances melting of ice shelves and reduces formation of Antarctic Bottom Water. *Science Advances*, *4*(4), eaap9467. doi: 10.1126/sciadv.aap9467

Smith, B., Fricker, H. A., Gardner, A. S., Medley, B., Nilsson, J., Paolo, F. S., … Zwally, H. J. (2020). Pervasive ice sheet mass loss reflects competing ocean and atmosphere processes. *Science*, *368*(6496), 1239–1242. doi:

10.1126/science.aaz5845

Snow, K., Hogg, A. M., Sloyan, B. M., & Downes, S. M. (2016). Sensitivity of Antarctic Bottom Water to Changes in Surface Buoyancy fluxes. *J. Climate*, *29*(1), 313–330. doi: 10.1175/JCLI-D-15-0467.1

Stammer, D. (2008). Response of the global ocean to Greenland and Antarctic ice melting. *J. Geophys. Res.*, *113*(C6), C06022. doi: 10.1029/2006JC004079

Stouffer, R. J., Seidov, D., & Haupt, B. J. (2007). Climate response to external sources of freshwater: North Atlantic versus the Southern Ocean. *J. Climate*, *20*(3), 436–448. doi: 10.1175/JCLI4015.1

Taylor, K. E., Stouffer, R. J., & Meehl, G. A. (2011). An overview of CMIP5 and the experiment design. *Bull. Amer. Meteor. Soc.*, *93*(4), 485–498. doi: 10.1175/BAMS-D-11-00094.1

Todd, A., Zanna, L., Couldrey, M., Gregory, J., Wu, Q., Church, J. A., … Zhang, X. (2020). Ocean-only FAFMIP: Understanding regional patterns of ocean heat content and dynamic sea level change. *J. Adv. In Modeling Earth Systems*, *12*, e2019MS002027. doi: 10.1029/2019MS002027

Velicogna, I., & Wahr, J. (2013). Time-variable gravity observations of ice sheet mass balance: Precision and limitations of the GRACE satellite data. *Geophys. Res. Lett.*, *40*(12), 3055–3063. doi: 10.1002/grl.50527

Yin, J. J., Griffies, S. M., & Stouffer, R. J. (2010). Spatial variability of sea level rise in twenty-first century projections. *J. Climate*, *23*(17), 4585–4607. doi: 10.1175/2010JCLI3533.1

Zika, J. D., Skliris, N., Blaker, A. T., Marsh, R., Nurser, A. J. G., & Josey, S. A. (2018). Improved estimates of water cycle change from ocean salinity: the key role of ocean warming. *Environmental Res. Lett.*, *13*(7), 074036. doi: 10.1088/1748-9326/aace42

Supporting Information

S1 Description of simulation

We initially run the model for 300 years. We then test the sensitivity of model parameters that control mixing, diffusion, and convection, and we adjust the parameters in order to simulate a relatively realistic ocean circulation including the global residual meridional overturning circulation. Specifically, we change the parameter “diffKrT/S”, which is the background vertical diffusivity and was set by default during the sensitivity testing to vary with depth between 0.1×10^{-4} m^{2}s^{-2} and 1.5×10^{-4} m^{2}s^{-2}, to instead vary with depth between 0.5×10^{-4} m^{2}s^{-2} and 1.75×10^{-4} m^{2}s^{-2} in the Spin-up simulation.

We then run the Spin-up simulation until the end of year 7974. We find that the global volume-mean temperature and salinity evolve approximately exponentially toward their equilibrium values with e-folding timescales of 1090 years and 1340 years, respectively, after the first few thousand years (Fig. S2).

The Control, Surface, and Deep simulations are branched from the beginning of year 7540 of the Spin-up simulation. We set the Spin-up simulation to save daily output of the temperature and salinity relaxation fields during years 7540-7599, which we use to generate a 60-year cycle of daily fluxes. Note that the simulations with specified fluxes use the “Qnet” and “saltflux” surface forcing options in MITgcm. This requires changing the sign of the Spin-up simulation output to be used as input in the simulations with specified fluxes. In order to preserve the daily-mean values when the model linearly interpolates between values at the midpoint of each day, we use a process called “diddling” to adjust the daily data (Killworth, 1996). The perturbations in the Surface and Deep simulations are added as water at 0 psu and 0°C using the “AddMass” option in MITgcm.

We select year 7540 as the start time of the simulations with specified fluxes because (i) it allows the Spin-up simulation to reach a relatively high level of equilibration (SI Fig. S2) and (ii) the 60-year mean during years 7540–7599 of the global-means of both flux fields is approximately zero (SI Fig. S3). The latter condition is important because the global volume-mean temperature and salinity in the Control simulation evolves at a constant rate that is set by the global-mean values of these fixed surface fluxes. The drift in volume-mean temperature and salinity in the Control simulation is 2.5×10^{-5} K/yr and 7×10^{-6} g/kg/yr, which is considerably smaller than some other studies that used a similar method (e.g., 0.02 K/yr and 0.02 g/kg/yr in Zika et al., 2018).

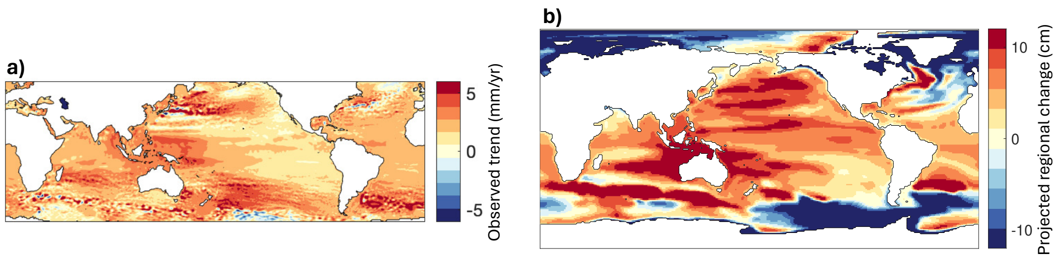

Figure S1. Maps of observed and projected regional sea level changes. (a) Observed sea level trends during 1993 to 2018, computed using the AVISO satellite altimetry dataset (Ducet et al., 2000). Only the latitude range 60°S–60°N is plotted due to limited data coverage in higher latitudes. (b) Projected future regional pattern of sea level change generated using the GFDL-ESM2M simulation of the CMIP5 scenario RCP 4.5, shown as the average during years 2090-2099 compared with 2006-2015. The simulation results include dynamic contributions due to changes in ocean density and mass redistribution, as well as land ice and terrestrial water components which are calculated using a separate modeling framework (for details see main text as well as Church et al., 2013). Here the global-mean sea level rise, which is 41 cm, is subtracted from the future projection in order to better illustrate the regional patterns.

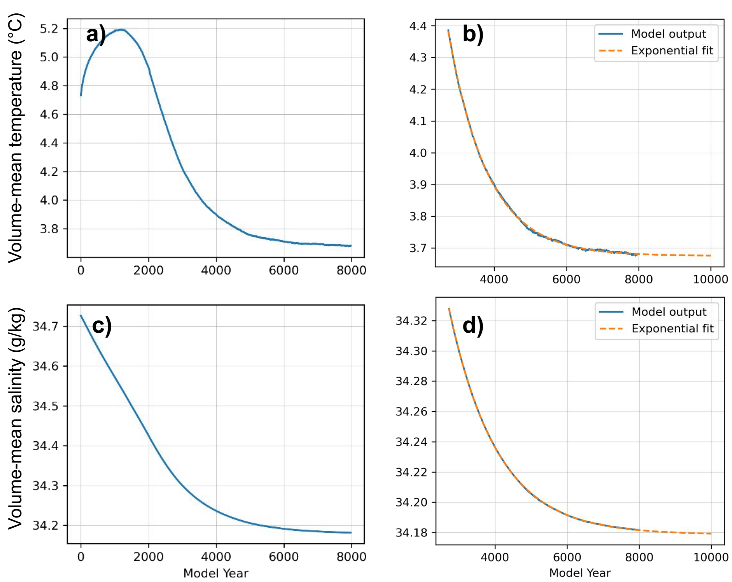

Figure S2. Evolution of (a,b) temperature and (c,d) salinity during (a,c) the entire Spin-up simulation and (b,d) the final 5000 years of the 7975-year Spin-up simulation. The dashed lines show exponential fits, with e-folding timescales of 1090 years for temperature and 1340 years for salinity.

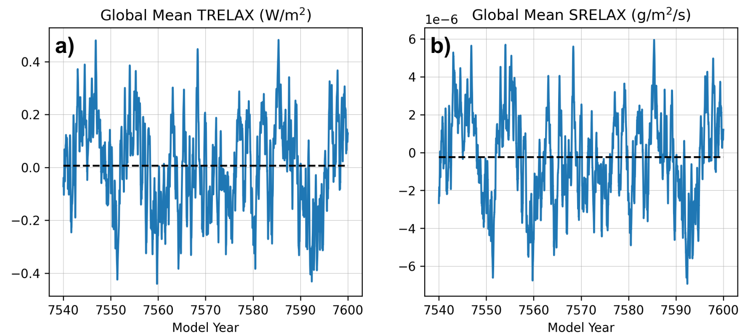

Figure S3. Evolution of the global-mean value of (a) the temperature flux and (b) the salinity flux due to the surface relaxation conditions during years 7540-7599 of the Spin-up simulation. The black dashed line shows the time average. The fluxes during the time period plotted here are used as the fixed surface fluxes in the Control, Surface, and Deep simulations.

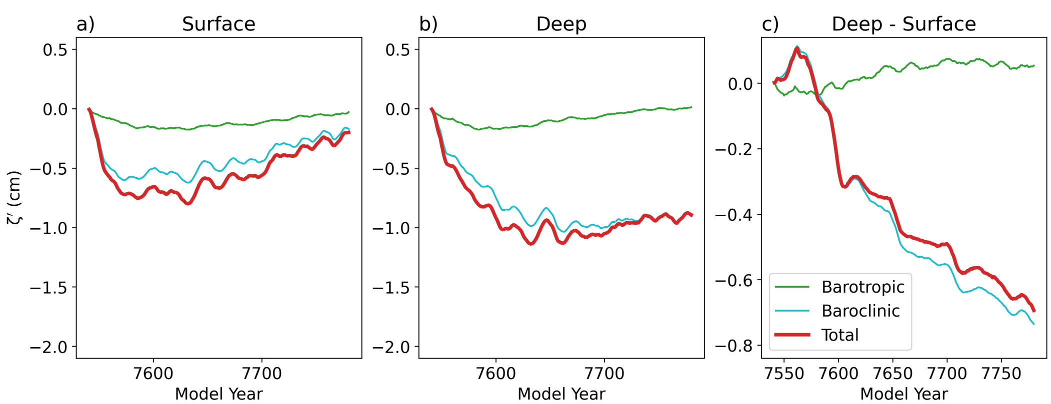

Figure S4. As in Fig. 4, but using a decomposition of Northern Hemisphere dynamic sea level anomaly ζ' into components associated with barotropic and baroclinic circulation changes (McWilliams et al., 2023), rather than components associated with mass redistribution and steric changes (Gill & Niiler, 1973; Yin et al., 2010; Griffies et al., 2014; Gregory et al., 2019). Here, only the sea level away from the continental shelves is decomposed, as per the requirements in McWilliams et al. (2023).